Impacts of Ion-Pairing Effects on Linear and Nonlinear Photophysical Properties of Polymethines Dyes

Simon Pascal, San-Hui Chi, Joseph W Perry, Chantal Andraud, Olivier Maury, S.-H Chi

Impacts of Ion-Pairing Effects on Linear and Nonlinear Photophysical Properties of Polymethines Dyes

Simon Pascal,*[a,b] San-Hui Chi,[c] Joseph W. Perry,[c] Chantal Andraud*[a] and Olivier Maury*[a]

[a] Dr. S. Pascal, Dr. C. Andraud, Dr. O. Maury
Laboratoire de Chimie
Univ. Lyon, ENS Lyon, CNRS, Université Lyon 1
46 Allée d'Italie, 69364 Lyon, France
E-mail: chantal.andraud@ens-lyon.fr; olivier.maury@ens-lyon.fr

[b] Dr. S. Pascal, current adress:
Aix Marseille Univ, CNRS UMR 7325, CINaM
Campus de Luminy, case 913
13288 Marseille cedex 09, France
E-mail: pascal@cinam.univ-mrs.fr

[c] Dr. S.-H. Chi, Prof. J. Perry
School of Chemistry and Biochemistry
Center for Organic Photonics and Electronics
Georgia Institute of Technology
901 Atlantic Drive NW, Atlanta, Georgia 30332-0400, United States

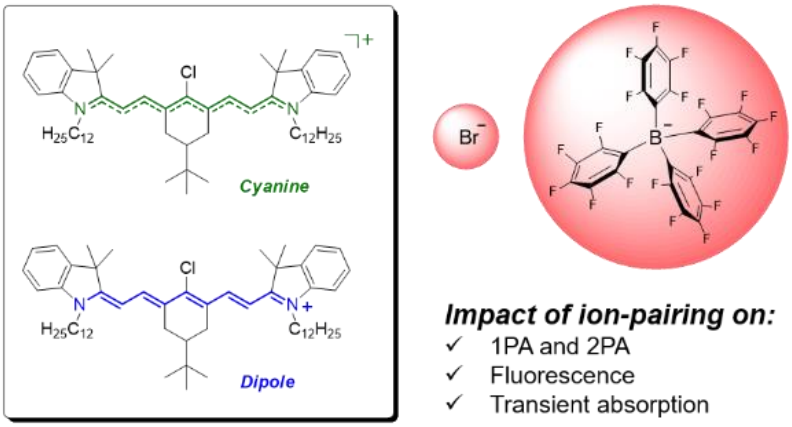

Abstract: The two-photon absorption (2PA) and photophysics of heptamethine dyes featuring *cyanine* or *dipolar* electronic structures has been compared for the first time. The perfectly delocalized *cyanine* system is classically characterized by a two-photon transition matching the vibronic component of its lower energy absorption band. The *dipolar* species is generated by ion-pairing with a hard counterion in non-dissociating solvent and displays significant optical properties modifications, including dramatic hypochromic shift of absorption, weaker emission and 2PA matching the lower energy transition, thus revealing symmetry breaking within the polymethine electronic structure.

Introduction

Polymethines are a fascinating class of dyes in which a positive (or negative) charge is delocalized over the conjugated skeleton comprised of an odd number of Csp^2 atoms between two electron donating (and/or withdrawing) moieties. In the most interested *cyanine state* (form I, Figure 1), sometimes also called *ideal polymethine state,* the charge is delocalized over the entire conjugated backbone with vanished bond-length alternation (BLA, *i.e.* the difference between two adjoining Csp^2-Csp^2 bonds) and results in the distinctive absorption spectrum that has been extensively studied over the last decades. As shown in Figure 1, the absorption spectrum features a sharp, intense absorption band with a characteristic high-energy shoulder. This strong absorption can be enhanced or redshifted into the near-infrared (NIR) spectral range, such as in heptamethine derivatives, by simple engineering of the extremities or elongation of the conjugated pathways.[1-3] The *cyanine* emission exhibits a very small Stokes shift, signature of a minimal excited state molecular relaxation.

Within the cyanine family, pentamethines and heptamethines with five- and seven-carbon bridges, respectively, have attracted much attention for applications in bio-imaging and material science.[4-9] Commercially available indocyanine green, is largely used for *in vivo* bio-imaging applications or further bioconjugation.[11, 12] Some polymethines have also been extensively studied for nonlinear optical applications, such as all-optical signal processing or optical limiting, in the telecommunication wavelengths range [1.3-1.5 µm].[13-19] The development of such applications requires the optimization of the optical properties of the material through a precise molecular-level manipulation of the electronic structure of the polymethine dyes, by controlling the nature of the counterion.[16, 20-22] In fact, it is well known that polymethines can present other ground state electronic structures, as the charge is localized at one extremity, breaking the symmetry of the conjugated backbone and forming a *dipolar* chromophore.[23] This electronic state, also known as *polyene-like state*, features a broad absorption band (form II, Figure 1). This phenomenon, generally referred to as "crossing the cyanine limit" in the literature, can be achieved by (i) the lengthening of the conjugated skeleton,[24-26] (ii) the modification of the donor end group,[19, 27] (iii) of solvent polarity[28] or (iv) monitoring ion-pairing effects.[10, 29] Furthermore, the existence of a third ground state electronic structure called *bis-dipole* has also been described as the charge is localized on the central Csp^2 atom of the bridge under the influence of vicinal electron donating moieties.[30] In a general way, the transition from one state to another is monitored using absorption spectroscopy, which provides a strong indication of each electronic structure. Herein, we generalized this study and examined in detail the impact of the ground state electronic structure on other spectroscopic features like emission, nonlinear absorption and transient absorption spectroscopic properties.

In particular, the transition from *cyanine* to *dipole* electronic structures involves a drastic modification of the electronic density distribution over the conjugated bridge. Consequently, a significant impact on the molecular polarizability and hence on the nonlinear optical properties is anticipated, as theoretically predicted in the case of symmetry breaking by ion-pairing.[20, 31, 32] For this purpose, we prepared the heptamethine **1** featuring lipophilic dodecyl substituents to ensure optimal solubility in classical organic solvents in association with small (Br^-) or bulky ($B(C_6F_5)_4^-$) counterions (Figure 1). While the *cyanine* state is classically observed in chlorinated solvent with both counterions, the *dipolar* state is reached by ion-paring effect in nonpolar solvent (*e.g.* toluene) in the case of **1[Br]**. This fine control of the cyanine to dipole transition reveals the impact of the symmetry of the electronic distribution on a larger panel of photophysical properties.

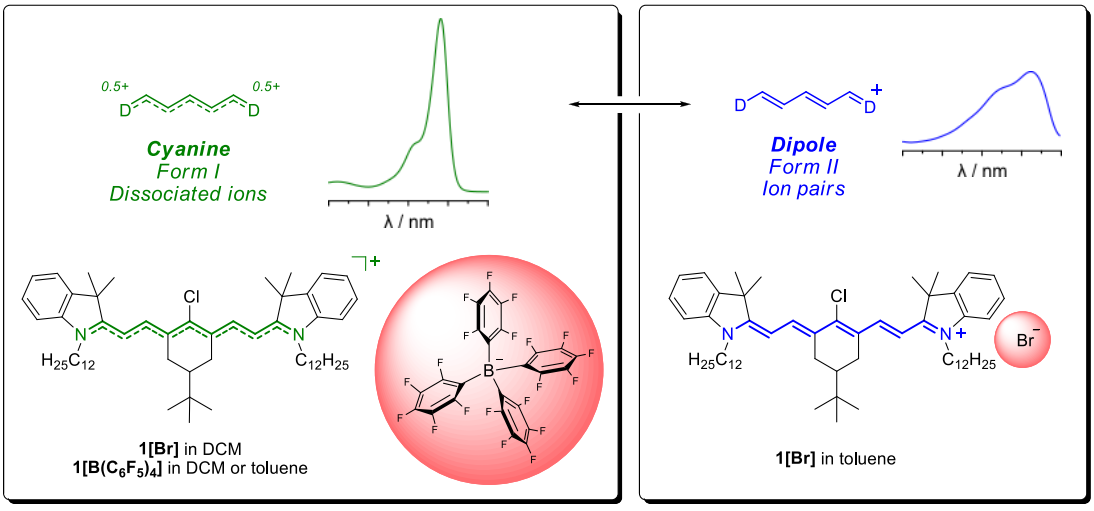

Figure 1. Representation of the *cyanine* and *dipolar* electronic structures of polymethine dyes with their corresponding absorption profiles, and illustration of the ion-pairing phenomenon within the heptamethine **1**, depending on the counterion and solvent natures.[10]

Results and Discussion

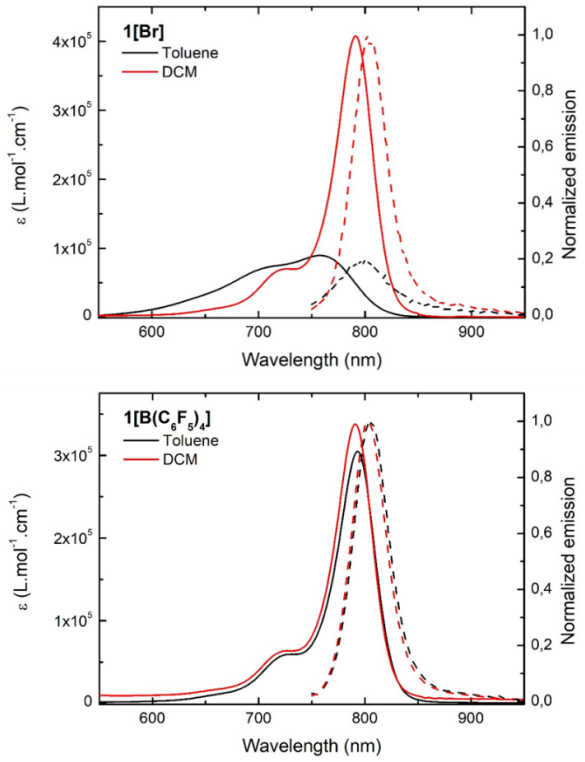

Figure 2. Absorption (plain line) and emission (dotted line) spectra of polymethines **1[Br]** (top) and **1[B(C$_6$F$_5$)$_4$]** (bottom) in toluene (black) and DCM (red).

Table 1. Optical and photo-induced kinetic properties of **1[Br]** and **1[B(C$_6$F$_5$)$_4$]** in toluene and DCM.

	1[Br]		**1[B(C$_6$F$_5$)$_4$]**	
	toluene	DCM	toluene	DCM
λ_{1PA}[a] / nm	758	791	793	791
ε / L.mol^{-1}.cm^{-1}	90000	408000	305000	338000
σ_{01}[a] / cm^2	3.4×10^{-16}	1.6×10^{-15}	1.2×10^{-15}	1.3×10^{-15}
λ_{em}[a] / nm	806	808	806	802
Φ	0.04	0.29	0.24	0.29
τ / ns	<0.4	1.3	1.2	1.3
λ_{2PA}[a][b] / nm	700	723	720	726
δ[a][b] / GM	310	510	410	510
$\lambda_{1\text{-}5}$[c] / nm	525	525	519	521
$\sigma_{1\text{-}5}$[c] / cm^2	8.1×10^{-17}	9.5×10^{-17}	4.5×10^{-17}	11×10^{-17}
τ_{gain} / ns	0.27	1.4	1.1	1.2

[a] The value is reported at spectral maximum, λ_{1PA}. [b] The value is reported based on the result of ND-2PA measurements. The ND-2PA cross section is converted to the degenerated two-photon cross section as $\delta_{ND} = 2\delta_D$. [c] The value is reported at spectral maximum, 525 nm, corresponding to the S_1-S_5 transition.

The improved solubility of heptamethine **1** allows to study its photophysical properties in dichloromethane (DCM, dissociating solvent) but also in a non-dissociating apolar solvent like toluene with both counterions. In the case of the bulky [B(C$_6$F$_5$)$_4$] counterion, no ion-pairing occurs in nonpolar solvent, thus the absorption and emission spectra of **1[B(C$_6$F$_5$)$_4$]** are identical in both solvents with a small Stokes shift of *ca.* 200 cm^{-1} (Figure 2 and Table 1), as previously reported.[10] The absorption profile is typical of a polymethine in the *cyanine* state with a sharp and intense transition featuring a characteristic high-energy vibronic shoulder. The emission band is the perfect mirror of the absorption band with a significant quantum yield in both solvents (0.24 in toluene, 0.29 in DCM) and identical luminescence lifetimes. In marked contrast, **1[Br]** featuring a smaller counterion presents a completely different behaviour in the two solvents. We first checked that **1[Br]** follows the Beer-Lambert law in both solvents ruling out any risk of aggregation (see supporting information Figures S1-S3). Heptamethine **1[Br]** shows the characteristics of a *cyanine* state in DCM and the ion pair is fully dissociated. Consequently, both absorption and emission spectra are identical to that of **1[B(C$_6$F$_5$)$_4$]**. On the contrary, in toluene, the broad absorption band indicates a loss of the *cyanine* character. The strong optical and structural similarities to the related push-pull chromophore indicate that an inseparable ion-pair is formed in a non-dissociating solvent. The bromide anion polarizes the conjugated skeleton and the charge is localized at one extremity (Figure 1).[10] In other words, a push-pull structure with one electron-donating indole and one electro-withdrawing indolenium moieties is obtained for **1[Br]** in toluene. It is worth noting that, the emission of **1[Br]** in toluene is very weak with a dramatic decrease of the fluorescence quantum yield (0.04) and luminescence lifetime (Table 1). Interestingly, the emission profile is not the mirror image of the absorption one, but is comparable to a *cyanine* emission as that of **1[B(C$_6$F$_5$)$_4$]** (Figure 2). This indicates that in the excited state, **1[Br]** in toluene presents a *cyanine*-like structure, with however a reduced fluorescence lifetime, suggesting faster non-radiative deexcitation process in the associated ion-pair (*vide infra*).

To monitor the *cyanine*-to-*dipole* transition and the formation of the ion pairs, the absorption and emission spectroscopies of **1[Br]** were studied in mixtures of DCM and toluene (Figure 3). As the proportion of toluene increases, it can be noticed that the *cyanine*-type absorption band gradually reduced. This observation reveals a dynamic association equilibrium between the heptamethine and its counterion in solution. The gradually broadening of the absorption band is accompanied by the decrease of the fluorescence quantum yields which accounts that a combination of polymethine of *cyanine* and *dipolar* forms can be found in solution (Table 2). It is noteworthy that there are minor changes in emission maxima and full-width at half-maximum (FWHM), regardless the mixing ratio of DCM and toluene, and the excitation spectra are all superimposable to the corresponding absorption spectra.[33] These observations again suggest that the observed emission can be attributed to *cyanine*-type excited state in **1[Br]**. The roles of *cyanine*- and *dipole*-type electronic structures effect on the nonlinear two-photon absorption properties are studied

Table 2. Photophysical data for compound **1[Br]** in mixtures of DCM and toluene.

DCM : toluene	λ_{abs} / nm	λ_{em} / nm	Φ	τ / ns	$FWHM^{abs}$ / cm^{-1}	$FWHM^{em}$ / cm^{-1}
0 : 1	758	806	0.04	< 0.4	2337	834
2 : 8	777	811	0.04	0.5	1956	656
4 : 6	792	811	0.08	1.1	910	650
6 : 4	794	811	0.16	1.3	655	607
8 : 2	792	810	0.17	1.2	657	623
1 : 0	791	808	0.29	1.3	658	572

using non-degenerate two-photon absorption spectroscopy (ND-2PA) and open-aperture z-scan to characterize the 2PA spectra and the magnitude of 2PA cross sections, respectively.

The 2PA and excited state absorption (ESA) spectra of heptamethines **1[Br_4]** and **1[$B(C_6F_5)_4$]** in DCM and toluene are shown in Figure 4 and the corresponding optical parameters are listed in Table 1. As indicated in Figure 2, both heptamethines in DCM exhibit *cyanine*-type ground state electronic structure. According to the selection rule, the lowest-energy ground state transition of a polymethine is two-photon forbidden due to the symmetry. Both heptamethines show blue-shifted 2PA maxima, in relative to the linear absorption maxima that overlap with the vibronic side band near 720 nm with sizable cross sections about 500 GM. This behaviour is assigned to the vibronic-allowed 2PA of the heptamethine.[15] These measurements confirmed that the nature of the counter-ion has minor impact on the 2PA properties in a dissociating solvent like DCM. In toluene, **1[$B(C_6F_5)_4$]** bearing the bulky anion shows the signature of vibronic-allowed 2PA near 720 nm with slightly reduced cross section of ~400 GM. In contrast, **1[Br]** in toluene shows broaden, blue-shifted 2PA spectrum (~700 nm) that overlaps the 1PA spectrum with a further reduced 2PA cross section of ~300 GM (Figure 5). The observed result again supports the previous discussion concerning the ground state electronic symmetry breaking due to ion-pairing effect and confirms that **1[Br]** exhibits predominately a non-centrosymmetric *dipolar* electronic structure in nonpolar solvent.

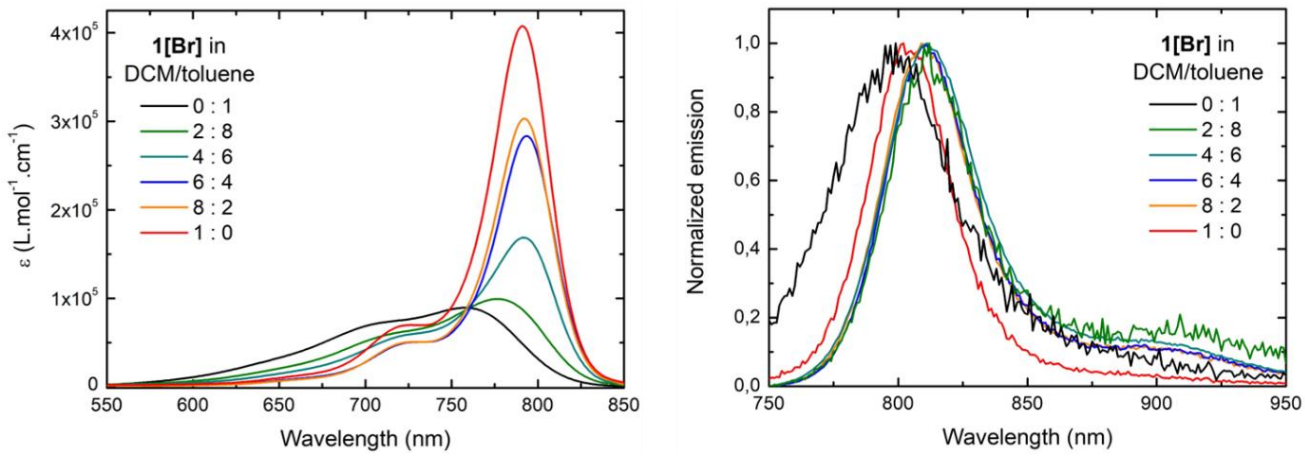

Figure 3. Absorption (left) and normalized emission (right) spectra recorded for **1[Br]** in mixtures of DCM and toluene.

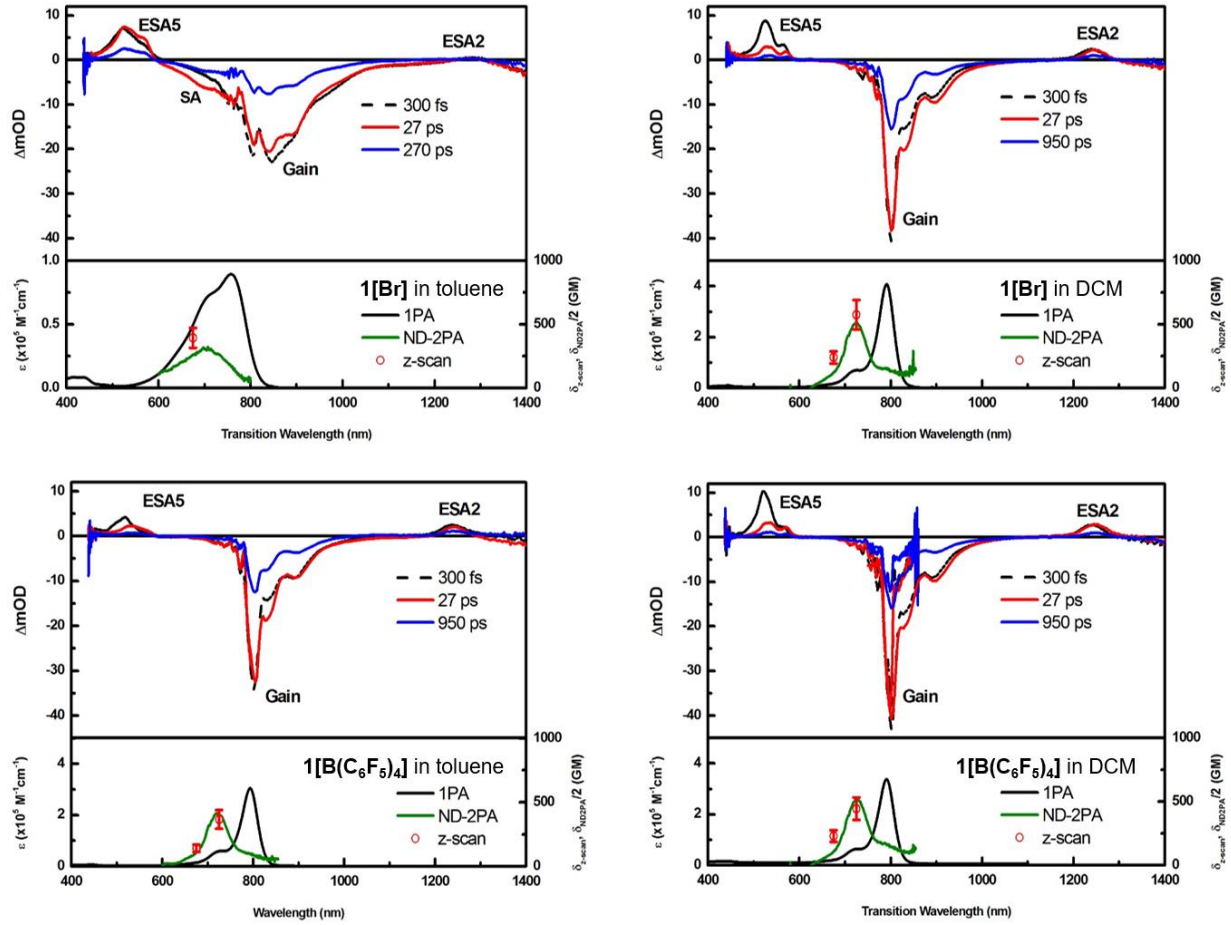

Figure 4. Linear, two-photon absorption, and transient absorption spectra of **1[Br]** and **1[B(C$_6$F$_5$)$_4$]** in toluene and DCM.

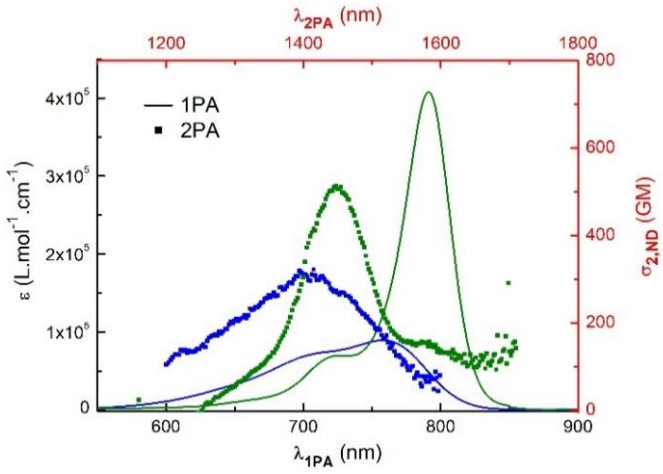

Figure 5. Linear (plain line) and two-photon (squares) absorptions of compounds **1[Br]** (blue) and **1[B(C$_6$F$_5$)$_4$]** (green) in toluene solution.

Ultrafast transient absorption spectroscopy was applied to observe the photophysics and establish structure-property relationships (Figures 4 and 6). In all cases, the stimulated emission (gain) is observed ca. 800 nm, accompanied with two ESA bands S_1-S_5 at 525 nm and S_1-S_2 in the NIR, which match well the transitions reported in the literature.[26] The stimulated emission confirms the fluorescence study, *i.e.* **1[Br]** in DCM and **1[B(C$_6$F$_5$)$_4$]** in both DCM and toluene show intense and narrow gain at 800 nm with lifetime ~1.1-1.4 ns, similar to literature reported value.[26, 34] In addition, the symmetry breaking of **1[Br]** in toluene is also observed and leads to reduced gain intensity and lifetime (270 ps). One can notice that the profile of the stimulated emission presents a broad and structure-less transition, with red-shifted peak *ca.* 840 nm.

The cross section of ESA was extracted by a numerical method of nonlinear beam propagation.[35] Concerning the NIR S_1-S_2 band, a slight difference can be observed in the case of **1[Br]** in toluene, but the signal is too weak to make any comment. The S_1-S_5 transition ($\lambda_{1\text{-}5}$) around 525 nm is more intense with cross section ($\sigma_{1\text{-}5}$) on the order of 1×10^{-16} cm^2, similar to the literature reported value.[26, 34] The size of cross sections S_1-S_5 of both **1[Br]** and **1[B(C$_6$F$_5$)$_4$]** in toluene are relatively smaller compared to that in DCM. The kinetic of the S_1-S_5 (Figure 6) confirms the emission lifetime tendency reported in Table 1 (see τ *vs* τ_{gain}), with values *ca.* 1.0-1.4 for cyanine forms and inferior to 0.4 ns for the dipolar form. It should be noted that the fast spike observed in the kinetic curve is due to the fast population of the excited state populations (depopulation of the ground state populations) stimulated by a white light continuum probe.

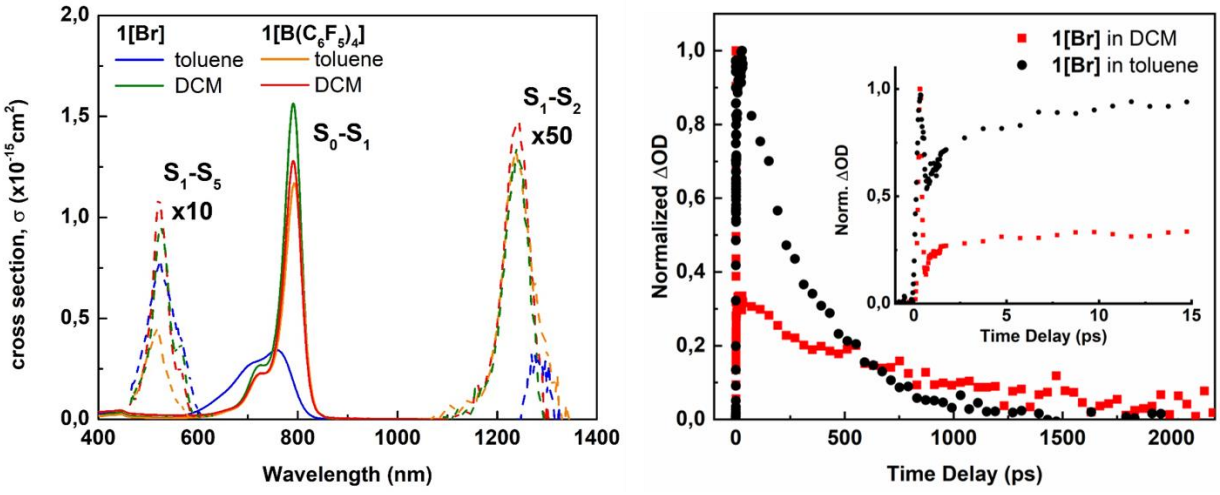

Figure 6. (Left) Linear (plain lines) and excited state absorption (dashed lines) cross sections of heptamethines **1[Br]** and **1[B(C$_6$F$_5$)$_4$]**. (Right) Kinetics of S_1-S_5 transition of **1[Br]** in DCM and toluene.

Conclusion

In conclusion, we studied the *cyanine-to-dipole* transition in heptamethine dyes using emission, nonlinear and transient absorption spectroscopies. The investigation of the fluorescence pointed out that both electronic structures give rise to an emission from a cyanine-type excited state. Moreover, the progressive transition between the *dipolar* and *cyanine* forms revealed a dynamic association equilibrium between the heptamethine and its counterion in solution. The establishment of a polyene-like electronic structure could be monitored for the first time with nonlinear absorption measurements, highlighting the overlap of the 1PA and 2PA transitions in the *dipolar* state in the NIR, due to the ground state symmetry breaking induced by ion-pairing.

Experimental Section

Synthetic procedures. The synthesis of heptamethine **1** was performed following a reported procedure.[36] NMR spectra were recorded at room temperature on a BRUKER® Avance operating at 500.1 MHz, 125.8 MHz and 188.8 MHz for ^{1}H, ^{13}C and ^{19}F, respectively. ^{13}C NMR signals were assigned using HSQC and HMBC experiments. Chemical shifts are listed in parts per million (δ, ppm) and are reported relative to residual solvent peaks being used as internal standard (for ^{1}H and ^{13}C respectively: $CDCl_3$: 7.26 and 77.2 ppm). Hydrogen atoms in equatorial or axial configuration are noted H_{eq} or H_{ax}, respectively. High resolution mass spectrometry measurements were performed at the *Centre Commun de Spectrometrie de Masse* (Villeurbanne, France).
Synthesis of compound **1[B(C$_6$F$_5$)$_4$]***:* a Schlenk tube was charged with 50 mg of heptamethine **1[Br]** (0.05 mmol, 1 equiv), 47 mg of lithium tetrakis(pentafluorophenyl)borate ethyletherate (0.05 mmol, 1 equiv) and added by 10 mL of anhydrous dichloromethane. The solution was stirred for 30 minutes at 25 °C, then washed with water (2 x 10 mL), dried over anhydrous Na_2SO_4 and concentrated under reduced pressure. After filtration trough a silicagel plug with dichloromethane, the product was isolated as a green solid in a 98% yield (80 mg). ^{1}H NMR ($CDCl_3$, 500 MHz): δ = 8.39 (d, ^{3}J = 14 Hz, 2H, =CH), 7.36 (d, ^3J = 8 Hz, 4H, CH_{Ar}), 7.25 (d, ^3J = 8 Hz, 2H, CH_{Ar}), 7.06 (d, ^3J = 8 Hz, 2H, CH_{Ar}), 6.05 (d, ^3J = 14 Hz, 2H, =CH), 3.97 (t, ^3J = 7 Hz, 4H, N-CH_2), 2.84 (dd, ^2J = 14 Hz, ^3J = 3 Hz, 2H, H_{eq}), 2.19 (dd, ^2J = 14 Hz, ^3J = 14 Hz, 2H, H_{ax}), 1.82 (quint, ^3J = 7 Hz, 4H, CH_2), 1.70 (s, 6H, $C(CH_3)_2$), 1.69 (s, 6H, $C(CH_3)_2$), 1.60 (m, 1H, CH), 1.44 – 1.33 (m, 8H, CH_2), 1.23 (m, 28H, CH_2), 1.04 (s, 9H, $C(CH_3)_3$), 0.87 (t, ^3J = 7 Hz, 6H, CH_3). ^{13}C NMR ($CDCl_3$, 126 MHz): δ = 172.9 (C), 151.5 (C), 149.3 (m, C), 147.3 (m, C), 145.0 (CH), 142.0 (C), 141.2 (C), 137.3 (m, C), 135.5 (m, C), 129.0 (CH), 127.2 (C), 125.8 (CH), 122.6 (CH), 110.7 (CH), 100.5 (CH), 49.6 (C), 44.6 (NCH_2), 42.3 (CH), 32.4 (C), 32.1 (CH_2), 29.7 (2 CH_2 or 2 CH_3), 29.6 (CH_2 or CH_3), 29.6 (CH_2 or CH_3), 29.4 (CH_2 or CH_3), 29.3 (CH_2 or CH_3), 28.2 (CH_2 or CH_3), 28.1 (CH_2 or CH_3), 27.4 (2 CH_2 or 2 CH_3), 27.2 (CH_2 or CH_3), 22.8 (CH_2), 14.2 (CH_3). ^{19}F NMR ($CDCl_3$, 189 MHz): δ = -132.5 (d, $J_{F\text{-}F}$ = 11 Hz, 2F), -163.3 (t, $J_{F\text{-}F}$ = 20 Hz, 1F), -166.9 (t, $J_{F\text{-}F}$ = 18 Hz, 2F). UV-Vis (CH_2Cl_2): λ_{max} = 791 nm (ε_{max} = 338000 L.mol^{-1}.cm^{-1}). HRMS (ESI+): $[M]^+$ = 847.6596 (calculated for $C_{58}H_{88}ClN_2$: 847.6631).

Linear absorption and luminescence. Absorption spectra were recorded on a JASCO V-650 spectrophotometer in diluted solution (*ca.* 10^{-6} mol.L^{-1}) using spectrophotometric grade solvents. Molar extinction coefficients (ε) were precisely determined at least two times and for different concentrations of **1[Br]** in DCM or toluene to verify that this compound follows the Beer-Lambert law within the experimental error (see Figures S1-S3 in Supporting Information). Emission spectra were measured using a Horiba-Jobin-Yvon Fluorolog-3 iHR320 fluorimeter. Fluorescence quantum yields *Q* were measured in diluted solutions with an absorbance lower than 0.1 using the following equation $Q_x/Q_r = [A_r(\lambda)/A_x(\lambda)][n_x^2/n_r^2][D_x/D_r]$ were *A* is the absorbance at the excitation wavelength (λ), n the refractive index and *D* the integrated luminescence intensity. "r" and "x" stand for reference and sample. The fluorescence quantum yields were measured relative to IR-125 in DMSO (Φ = 0.13). Excitation of reference and sample compounds was performed at the same wavelength. Short luminescence decay was monitored with the TC-SPC Horiba apparatus using Ludox in distilled water to determine the instrumental response function used for deconvolution. Excitation was performed using NanoLEDs, with

model 740 (732 nm; 1.3 ns). The deconvolution was performed using the DAS6 fluorescence-decay analysis software.

Two-photon and transient absorptions. All solutions were prepared in spectroscopic grade DCM (Acros Organics) with the averaged concentration of ~0.5-1.5 mM for ND-2PA and z-scan measurements and ~10-100 μM, to obtain optical densities between 0.6-1, for transient absorption (TA) spectroscopy. All samples were stirred continuously during measurements in 2 mm path-length fused silica cuvettes. The two-photon absorption (2PA) spectra were mapped with femtosecond-pulsed ND-2PA spectrometer[34] and the 2PA absorption cross sections, δ in GM, were confirmed with femtosecond-pulsed open aperture z-scan techniques. For ND-2PA measurements, excitation wavelengths of 1800 and a white light continuum (WLC) probe ranging from 950-1600 nm were selected to acquire the ND-2PA spectra from transition wavelength of 620-850 nm. For z-scan measurements, a near Gaussian beam at 1450 and 1350 nm with $M^2 < 1.1$, $\omega(HW_{1/e2})$ ~ 50 μm, and $\tau p(HW_{1/e})$ ~ 75 fs was used. The excitation irradiance ranges from 30 – 120 GW/cm^2. By definition, the ND-2PA measured two-photon cross section (δ_{ND}) should be 2 times larger than the z-scan measured degenerated two-photon cross section (δ_D). Femtosecond TA spectra and kinetic traces were measured with a commercially available broadband pump-probe spectrometer (HELIOS, Ultrafast Systems LLC) using a femtosecond Ti:Sapphire regenerative amplifier laser source (Solstice, Spectra-Physics, 800-nm, 3.7-W average power, 100-fs pulse width, 1-KHz repetition rate) and a computer-controlled optical parametric amplifier (OPA) (TOPAS, Spectra-Physics, wavelength range: 266-2290 nm, pulse width: ~75 fs HW1/e) pumped by the amplified laser. The excitation wavelength of 780 nm was generated using the output of OPA. The white-light continuum (WLC, 400-1600 nm) probe beam was produced by focusing less than 5% of the 800 nm amplified beam into a nonlinear crystal in the Helios. A chirp correction function for the WLC probe was determined using measurements of the non-degenerate nonlinear response of tetrahydrofuran and was applied to all transient spectra.[37]

Keywords: cyanine • polymethine • two-photon absorption • spectroscopy • near-infrared dyes

[1] A. Mishra, R. K. Behera, P. K. Behera, B. K. Mishra, G. B. Behera, *Chem. Rev.* **2000**, *100*, 1973-2012.
[2] A. V. Kulinich, A. I. Aleksandr, *Russ. Chem. Rev.* **2009**, *78*, 141.
[3] J. L. Bricks, A. D. Kachkovskii, Y. L. Slominskii, A. O. Gerasov, S. V. Popov, *Dyes Pigm.* **2015**, *121*, 238-255.
[4] K. Kiyose, H. Kojima, T. Nagano, *Chem. Asian J.* **2008**, *3*, 506-515.
[5] G. Qian, Z. Y. Wang, *Chem. Asian J.* **2010**, *5*, 1006-1029.
[6] Z. Guo, S. Park, J. Yoon, I. Shin, *Chem. Soc. Rev.* **2014**, *43*, 16-29.
[7] P.-A. Bouit, D. Rauh, S. Neugebauer, J. L. Delgado, E. D. Piazza, S. p. Rigaut, O. Maury, C. Andraud, V. Dyakonov, N. Martin, *Org. Lett.* **2009**, *11*, 4806-4809.
[8] A. Pertegás, D. Tordera, J. J. Serrano-Pérez, E. Ortí, H. J. Bolink, *J. Am. Chem. Soc.* **2013**, *135*, 18008-18011.
[9] S. Seo, S. Pascal, C. Park, K. Shin, X. Yang, O. Maury, B. D. Sarwade, C. Andraud, E. Kim, *Chem. Sci.* **2014**, *5*, 1538-1544.
[10] P.-A. Bouit, C. Aronica, L. Toupet, B. Le Guennic, C. Andraud, O. Maury, *J. Am. Chem. Soc.* **2010**, *132*, 4328-4335.
[11] W. Sun, S. Guo, C. Hu, J. Fan, X. Peng, *Chem. Rev.* **2016**, *116*, 7768-7817.
[12] T.-C. Wang, F. Cochet, F. A. Facchini, L. Zaffaroni, C. Serba, S. Pascal, C. Andraud, A. Sala, F. Di Lorenzo, O. Maury, T. Huser, F. Peri, *Bioconjugate Chem.* **2019**, *30*, 1649-1657.
[13] P.-A. Bouit, G. Wetzel, G. Berginc, B. Loiseaux, L. Toupet, P. Feneyrou, Y. Bretonnière, K. Kamada, O. Maury, C. Andraud, *Chem. Mater.* **2007**, *19*, 5325-5335.
[14] J. M. Hales, J. Matichak, S. Barlow, S. Ohira, K. Yesudas, J.-L. Brédas, J. W. Perry, S. R. Marder, *Science*. **2010**, *327*, 1485-1488.
[15] Q. Bellier, N. S. Makarov, P.-A. Bouit, S. Rigaut, K. Kamada, P. Feneyrou, G. Berginc, O. Maury, J. W. Perry, C. Andraud, *Phys. Chem. Chem. Phys.* **2012**, *14*, 15299-15307.
[16] J. M. Hales, S. Barlow, H. Kim, S. Mukhopadhyay, J.-L. Brédas, J. W. Perry, S. R. Marder, *Chem. Mater.* **2013**, *26*, 549-560.
[17] S. Barlow, J.-L. Bredas, Y. A. Getmanenko, R. L. Gieseking, J. M. Hales, H. Kim, S. R. Marder, J. W. Perry, C. Risko, Y. Zhang, *Mater. Horiz.* **2014**, *1*, 577-581.
[18] W. Bentoumi, J.-C. Mulatier, P.-A. Bouit, O. Maury, A. Barsella, J.-P. Vola, E. Chastaing, L. Divay, F. Soyer, P. Le Barny, Y. Bretonnière, C. Andraud, *Chem. Eur. J.* **2014**, *20*, 8909-8913.
[19] S. Pascal, Y. A. Getmanenko, Y. Zhang, I. Davydenko, M. H. Ngo, G. Pilet, S. Redon, Y. Bretonnière, O. Maury, I. Ledoux-Rak, S. Barlow, S. R. Marder, C. Andraud, *Chem. Mater.* **2018**, *30*, 3410-3418.
[20] S. Mukhopadhyay, C. Risko, S. R. Marder, J.-L. Bredas, *Chem. Sci.* **2012**, *3*, 3103-3112.
[21] A. C. Véron, H. Zhang, A. Linden, F. Nüesch, J. Heier, R. Hany, T. Geiger, *Org. Lett.* **2014**, *16*, 1044-1047.
[22] R. L. Gieseking, S. Mukhopadhyay, C. Risko, S. R. Marder, J.-L. Brédas, *Adv. Mater.* **2014**, *26*, 68-84.
[23] S. Pascal, A. Haefele, C. Monnereau, A. Charaf-Eddin, D. Jacquemin, B. Le Guennic, O. Maury, C. Andraud, *Proc. SPIE*. **2014**, *9253A*, 1-11.
[24] L. G. S. Brooker, R. H. Sprague, C. P. Smyth, G. L. Lewis, *J. Am. Chem. Soc.* **1940**, *62*, 1116-1125.
[25] L. M. Tolbert, X. Zhao *J. Am. Chem. Soc.* **1997**, *119*, 3253-3258.
[26] R. S. Lepkowicz, O. V. Przhonska, J. M. Hales, J. Fu, D. J. Hagan, E. W. Van Stryland, M. V. Bondar, Y. L. Slominsky, A. D. Kachkovski, *Chem. Phys.* **2004**, *305*, 259-270.
[27] F. Würthner, R. Wortmann, R. Matschiner, K. Lukaszuk, K. Meerholz, Y. De Nardin, R. Bittner, C. Bräuchle, R. Sens, *Angew. Chem. Int. Ed.* **1997**, *36*, 2765-2768.
[28] F. Würthner, G. Archetti, R. Schmidt, H.-G. Kuball, *Angew. Chem. Int. Ed.* **2008**, *47*, 4529-4532.
[29] S. Pascal, P.-A. Bouit, B. Le Guennic, S. Parola, O. Maury, C. Andraud, *Proc. SPIE*. **2013**, *86220F*, 1-9.
[30] S. Pascal, A. Haefele, C. Monnereau, A. Charaf-Eddin, D. Jacquemin, B. Le Guennic, C. Andraud, O. Maury, *J. Phys. Chem. A*. **2014**, *118*, 4038-4047.
[31] Y. Kada, *J. Mol. Struct.* **2019**, *1186*, 127-136.
[32] M. Eskandari, J. C. Roldao, J. Cerezo, B. Milián-Medina, J. Gierschner, *J. Am. Chem. Soc.* **2020**, *142*, 2835-2843.
[33] A. A. Ishchenko, *Russ. Chem. Rev.* **1991**, *60*, 865-884.
[34] R. A. Negres, O. V. Przhonska, D. J. Hagan, E. W. Van Stryland, M. V. Bondar, Y. L. Slominsky, A. D. Kachkovski, *IEEE J. Sel. Top. Quantum Electron.* **2001**, *7*, 849-863.
[35] S.-H. Chi, J. M. Hales, M. Cozzuol, C. Ochoa, M. Fitzpatrick, J. W. Perry, *Opt. Express*. **2009**, *17*, 22062-22072.
[36] S. Pascal, S. Denis-Quanquin, F. Appaix, A. Duperray, A. Grichine, B. Le Guennic, D. Jacquemin, J. Cuny, S.-H. Chi, J. W. Perry, B. van der Sanden, C. Monnereau, C. Andraud, O. Maury, *Chem. Sci.* **2017**, *8*, 381-394.
[37] S. A. Kovalenko, A. L. Dobryakov, J. Ruthmann, N. P. Ernsting, *Phys. Rev. A* **1999**, *59*, 2369-2384.